

SUNY-NTG-98-63; JYFL 98-17

e^+e^- yields in Pb+Au collisions at 158 AGeV/c: Assessment of baryonic contributions

Pasi Huovinen^{1,2} and Madappa Prakash¹

¹*Department of Physics & Astronomy, SUNY at Stony Brook, Stony Brook, USA*

²*Department of Physics, University of Jyväskylä, Finland*

(December 2, 2024)

Abstract

Using a hydrodynamic approach to describe Pb+Au collisions at 158 AGeV/c, we analyze e^+e^- yields from matter containing baryons in addition to mesons. We employ e^+e^- production rates from two independent calculations, which differ both in their input physics and in their absolute magnitudes, especially in the mass range where significant enhancements over expected backgrounds exist in the CERES data. Although the presence of baryons leads to significant enhancement of e^+e^- emission relative to that from mesons-only matter, the calculated results fall below the CERES data in the range $400 < M_{e^+e^-}/\text{MeV} < 600$, by a factor of 2-3. Since the calculated e^+e^- spectra are relatively insensitive to the equation of state for initial conditions that fit the observed hadronic spectra, either in-medium modifications of the e^+e^- sources more significant than so far considered, or the presence of hitherto unidentified additional sources of e^+e^- is indicated.

PACS number(s): 25.70.np, 12.38.Mh, 12.40.Ew, 47.75.+f

Electromagnetic signals from relativistic heavy-ion reactions directly probe the properties of the dense matter created during the collision, since, after production, their interactions with the evolving ambient matter are negligible [1]. The CERES collaboration at CERN, beginning with S+Au collisions at 200 AGeV/c and more recently with Pb+Au collisions at 158 AGeV/c, have reported dielectron (e^+e^-) yields that significantly exceed those from expected backgrounds [2,3]. For the pair invariant masses $M_{e^+e^-} < 2$ GeV, the background is chiefly from the decays of neutral mesons after they cease interacting with the produced matter. For nucleus-nucleus (AA) collisions, these backgrounds are estimated by extrapolating the measured yields from proton-proton (pp) and proton-nucleus (pA) collisions. Specifically, the reported average enhancements are 5.0 ± 0.7 (stat.) ± 2.0 (syst.) in the range $0.2 < M_{e^+e^-}/\text{GeV} < 1.5$ for the S+Au reaction and 3.5 ± 0.4 (stat.) ± 0.9 (syst.) in the range $0.2 < M_{e^+e^-}/\text{GeV} < 2$ for the Pb+Au reaction (hereafter the '95 data), respectively. In both cases, the pseudo-rapidity coverage was in the range $2.1 < \eta < 2.65$, the transverse momentum of e^+e^- pairs was restricted to $p_t > 200$ MeV, and only pairs with opening angle $\Theta_{ee} > 35$ mrad were accepted. The two experiments differed in that $\langle dN_{ch}/d\eta \rangle = 125$ for S+Au and $\langle dN_{ch}/d\eta \rangle = 220$ for Pb+Au. More recently, e^+e^- data from Pb+Au collisions with improved statistics and mass resolution have become available (hereafter the '96 data) in different charged particle multiplicity bins, including those for nearly central collisions [4]. To within two standard deviations, the '96 data are consistent with the '95 data and show similar enhancements, albeit at a somewhat lower level. To be specific, the average enhancement found was 2.6 ± 0.5 (stat.) ± 0.6 (syst.) in the range $0.25 < M_{e^+e^-}/\text{GeV} < 0.7$, with the enhancement increasing for more central collisions. For the same mass region and for the same background evaluation, the '95 data gives an average enhancement of 3.9 ± 0.9 (stat.) ± 0.9 (syst.). These enhancements over the expected background, particularly in the range $0.4 < M_{e^+e^-}/\text{GeV} < 0.6$ in both S+Au and Pb+Au reactions, are especially intriguing, since they have the potential to distinguish between competing theoretical scenarios concerning the in-medium properties of vector mesons, including

those of chiral restoration with increasing density and temperature.

The theoretical analysis of e^+e^- yields in AA collisions involves integrating the microscopic production rates over the space-time history of the produced matter and implementing the experimental cuts and resolution for an apposite comparison with the data. Since the dynamical evolution proceeds through stages consisting of both sub-hadronic and hadronic degrees of freedom, a knowledge of the relevant e^+e^- production rates is essential for a complete description. In this letter, we confront both the '95 and '96 data from $\text{Pb}+\text{Au}$ collisions with theoretical calculations which employ a hydrodynamic description for the space-time evolution and which use recently calculated e^+e^- emission rates in matter including baryons. Efforts are made to achieve a simultaneous description of both the hadronic and electromagnetic data. Special emphasis is placed on delineating the role baryons play in enhancing e^+e^- emissions relative to emissions in matter without baryons.

The dominant process in the Quark-Gluon Plasma (QGP) phase is the reaction $q\bar{q} \rightarrow e^+e^-$, for which we use the lowest order (in α and α_s) rates at a finite baryon chemical potential, summarized in Ref. [5]. Rates of $\mathcal{O}(\alpha^2\alpha_s)$ have significant contributions only in the mass region $M_{e^+e^-} < 500$ MeV, where the Dalitz decays of the final state mesons dominate, and are therefore not important. In all of the results to be reported, contributions from $q\bar{q}$ processes, whether they are from a pure QGP phase or a mixed phase, are dominated by those arising from the hadron gas phase.

In the hadron gas phase, prompt decays from vector, pseudoscalar, and axial vector mesons, as well as radiative decays and bremsstrahlung processes involving these mesons, all yield significant e^+e^- contributions in the invariant mass regions of interest here [6–9]. Through independent calculations, we have verified that the rates calculated by Gale and Lichard [7] (GL hereafter) and Lichard [8], who delineate a number of these processes, are consistent with the spectral-function approach of Steele, Yamagishi, and Zahed [10] (SYZ hereafter), who use experimentally extracted spectral functions and on-shell chiral reduction formulas coupled with a virial expansion scheme. Thus, in mesons-only matter, the GL and SYZ rates can be taken as a standard against which comparisons with other ap-

proaches [11–19], in which possible additional in-medium many-body effects are considered, may be made. These “standard” rates, when convolved with the space-time evolution of matter, in both transport and hydrodynamic approaches [20–24], have yielded results which are significantly below the measured yields in the region $400 < M_{e^+e^-}/\text{MeV} < 600$ in both S+Au and P+Au collisions. To date, only transport models [20–22], which incorporate substantial modifications of the in-medium properties, such as a sharply decreasing in-medium ρ -meson mass [25] or a significant widening of its width [11], have been able to account for the data.

In order to examine the extent to which baryons influence e^+e^- yields, we utilize rates from the independent calculations of Rapp, Urban, Buballa, and Wambach [13] (RUBW hereafter), and Steele, Yamagishi, and Zahed [10]. We have chosen these two rates, both because they represent a contrast in terms of the input physics and theoretical techniques employed, and because they differ significantly in the absolute magnitudes, especially for $M_{e^+e^-} \approx 500$ MeV, where the discrepancy between calculations and data is most significant.

The RUBW rates are based on a many-body approach in which phenomenological interactions are used to calculate the ρ -meson spectral function in matter containing baryons. In the first attempts using this approach [11,12], nucleon-hole and delta-hole excitations were found to substantially modify the ρ -meson spectral function from its form in vacuum and to significantly enhance the e^+e^- yields relative to those without such modifications. In subsequent works [13,14], however, these medium effects were constrained by photoabsorption data on protons and nuclei and on $\pi N \rightarrow \rho N$ production experiments. ρN interactions, particularly s-wave interactions involving the resonance $N^*(1520)$ and, to a lesser extent, p-wave interactions with the $N^*(1720)$, were found to result in a substantial broadening of the in-medium ρ -meson spectral function, albeit at a somewhat lower level than found in earlier works [11,12]. A theoretical discussion of the similarities and differences between the models of RUBW and those based on the Brown-Rho scaling of vector meson masses [25] may be found in Ref. [26].

Independently, SYZ have extended the spectral-function approach to include

baryons [10]. To leading order in the baryon density, the dilepton rates are proportional to the spin-averaged forward Compton scattering amplitude on the baryons by off-shell photons with $q^2 \geq 0$. While the photon rates can be determined directly from data by use of the optical theorem, the dilepton rates require additional theoretical considerations. SYZ use chiral constraints to determine the tree-level strong-interaction Lagrangian and preserve perturbative unitarity from an on-shell loop-expansion in $1/f_\pi$, which enforces current conservation and crossing symmetry. To one-loop, the rates are calculated without the use of any free parameter. The large contribution of the Δ to the Compton amplitude near threshold is taken into account by adding it as a unitarized tree term to the one-loop result. SYZ find that the dominant contribution arises from pion-nucleon interactions in the continuum and not from the Δ resonance.

The SYZ and RUBW rates are compared in Fig. 1, which illustrates the extent to which baryons can enhance the rates relative to those in mesons-only matter. For typical values of the temperature and baryon density of relevance here, the distinguishing features of the SYZ rates are: (1) Enhancements relative to the baryon-free case are of order 2-3 and are restricted to $M_{e^+e^-}/\text{MeV} < 500$. (2) The prominent signature at the ρ -meson vacuum mass persists at nearly all values of T and n_b . In contrast to SYZ, the two most striking features of the RUBW results are: (1) Rates are significantly larger than those of SYZ in the range $200 < M_{e^+e^-}/\text{MeV} < 600$. (2) The tell-tale signature at the ρ -meson vacuum mass is weakened, predominantly with increasing n_b . The differences between the results of these two calculations underscore the fact that a standard calculation of the rates in matter containing baryons, similar to those in mesons-only matter, is not yet available, which stresses the need to identify both common and distinguishing features between these two approaches.

As in Ref. [23], where a hydrodynamical description of 200 AGeV/c S+Au collisions was given, we place emphasis on the simultaneous description of the hadron and electromagnetic data in 158 AGeV/c Pb+Au collisions. Details of the hydrodynamical calculations may be found in Refs. [23,27]. Following these works, we assume that locally the system rapidly

achieves thermal and chemical equilibrium and parameterize it in terms of the various particle densities and fluid velocity. Our parametrization of the initial baryon density profile is motivated by the gross features of pp spectra (see Refs. [28,29]). The values of parameters describing the initial conditions are chosen to reproduce the measured hadron spectra. The densities and temperatures for the various stages of evolution are determined by specifying the equation of state (EOS), which enables a prediction of the e^+e^- emission from the various stages of the collision.

In view of the fact that hadronic data for the Pb+Au collision are not yet available, we have used the NA49 data from the Pb+Pb collision [30] to parameterize the initial conditions. The difference between the sizes of Pb and Au nuclei is small, and therefore one may justifiably expect the differences between the hadronic spectra in these two cases to be negligible. The initial conditions and the resulting hadronic spectra in Pb+Pb collisions are detailed in Ref. [27]. It must be noted, however, that NA49 uses a different centrality trigger from that used by CERES. Our calculations, which are tuned to reproduce the results of NA49, yield an average multiplicity of $\langle dN_{ch}/d\eta \rangle \cong 330$ within the CERES acceptance region. The CERES collaboration finds both the shape of the spectrum and the yield scaled with multiplicity to vary with multiplicity [31]. We have therefore opted here to compare our calculated results with the CERES data from nearly central collisions with $\langle dN_{ch}/d\eta \rangle = 350$. Comparisons of calculated results with the CERES data for noncentral collisions with different multiplicities and for different dielectron p_t cuts are essential for a comprehensive understanding, and will be reported separately.

For the most part, we show results of a baseline model calculated using the EOS labeled EOS D and initial state labeled IS 1 in Ref. [27]. For this EOS, the phase transition from a hadron gas to the QGP occurs at a temperature $T_c = 200$ MeV. The main reason for using an EOS with the somewhat high T_c of 200 MeV was to prolong the lifetime of the hadronic phase and make the changes in the emission rates due to the presence of baryons as distinct as possible from the case in which their contributions are ignored. Comparisons with the case in which $T_c = 165$ MeV (EOS A and IS 1 in Ref. [27]) will highlight the dependence on

phase transition temperature.

The hydrodynamical approach requires us to define a physical stage at which the system is sparse enough to be treated as noninteracting and consisting of freely streaming particles. For our baseline model, we define this so-called freeze-out as a space-time surface of constant energy density of $\epsilon_f = 0.15(0.069)$ GeV/fm³, which leads to an average freeze-out temperature of $T_f \cong 140(120)$ MeV. In Ref. [27], equivalent best fits to the hadron data were obtained using an EOS with $T_c = 200$ MeV combined with $T_f = 140$ MeV, and also an EOS with $T_c = 165$ MeV with $T_f = 120$ MeV. In the top and middle panels of Fig. 2, we compare the evolution of the temperature and baryon number density at the center of the fireball for these two cases. Note that, although the times for which the hadron gas phase lasts are nearly the same in both cases, its temperature is noticeably lower in the case in which T_c and T_f are smaller. As our results will show, this will have important implications for the total e^+e^- spectrum, which is calculated by integrating the emission rate in unit volume over the total space-time volume enclosed by the freeze-out surface.

In Fig. 3, we show the dileptons radiated during the lifetime of the fireball for the case in which $T_c(T_f) = 200(140)$ MeV. These results are folded with the cuts and resolution of CERES (for details, see Ref. [23]). The role of the baryons may be gauged by inspecting the time evolution of the baryon density in the fireball (Fig. 2). In the mixed phase, the average baryon density is $n_b = 0.4$ fm⁻³; i.e., 2.5 times the nuclear equilibrium density $n_0 \cong 0.16$ fm⁻³. However, the mixed phase lasts for a relatively short time and occupies too small a volume for a significant contribution to build up. Thus, in spite of the high temperatures in the mixed phase and the enhanced rates of both SYZ and RUBW with baryons, the mixed phase contributions to the total yield are small. The subleading contributions of the mixed phase cannot be used to discriminate between competing scenarios for the role of baryons.

The influence of baryons on e^+e^- production is dominant in the hadron gas phase, which dilutes rapidly due to hydrodynamic expansion. For $T_c = 200(165)$ MeV and $T_f = 140(120)$ MeV, the resulting average baryon density in the hadron gas phase of $n_b = 0.08(0.03)$ fm⁻³; i.e., $0.5(\sim 0.2) n_0$. The SYZ rates including baryons are about a factor of 2 larger than those

without baryons, but mostly below $M_{e^+e^-} = 400$ MeV. This translates to an enhancement of about a factor of two or less in this region, relative to the baryon-free case. The larger rates of RUBW result in enhancements of the thermal yield, even up to $M_{e^+e^-} = 300 - 600$ MeV, by a factor of about three relative to those in mesons-only matter.

In addition to e^+e^- pairs from the fireball, the measured yields contain contributions from vector meson decays after freeze-out. This background was calculated from the distributions of hadrons at freeze-out predicted by our model. Our calculated background is basically in agreement with the estimated CERES background and the experimentally measured hadron yields. The only exception is the ϕ/h^- ratio, which in experiments [32] is reported to be somewhat smaller than the ratio predicted in our calculations for $T_f = 140$ MeV. To achieve consistency with the data, we have suppressed the ϕ -yield in this case by a factor of 0.6. All other particle yields were assumed to arise from a thermally and chemically equilibrated (in the local sense) hadron gas. Fig. 4 shows a comparison of the individual contributions from the various hadrons after freeze-out for $T_c(T_f) = 200(140)$ MeV (dashed curves), and $T_c(T_f) = 165(120)$ MeV (dotted curves), respectively. These results also incorporate the experimental cuts and resolution of CERES. A notable feature in this comparison is the extent to which contributions from the $\omega \rightarrow e^+e^-$ decays are sensitive to the freeze-out temperatures. This is also reflected in the differences between the total contributions from the background at $T_f = 140$ MeV (thin solid curves) and $T_f = 120$ MeV (thin dashed curves) in the ω -mass region. We will return to the significance of this dependence later.

In Fig. 4, we also show the sum of the background and thermal (calculated with the RUBW rates for this figure) yields along with the data. The solid (dashed) curves show calculated results for $T_c = 200(165)$ MeV and $T_f = 140(120)$ MeV. The compensating contributions of the fireball and background components are evident in this comparison, inasmuch as their sums are nearly identical. A longer lifetime increases the thermal yield, but the background originating from a thermally and chemically equilibrated source diminishes with increasing lifetime. These compensating effects lead to the result that the total spectra for the two cases are similar, differing at most by a factor of 1.2 in the region where the

discrepancy between theory and experiment is significant. This highlights the fact that admissible changes in the phase transition and freeze-out temperatures play only a minor role in explaining the excess around $M_{e^+e^-} \cong 500$ MeV, but the precise values of the microscopic rates play a more significant role. One should bear in mind that both $T_c(T_f) = 200(140)$ MeV and $T_c(T_f) = 165(120)$ MeV produce equally good fits to the hadronic data. A more detailed discussion of the compensating effects of freeze-out and phase transition temperatures can be found in [27].

In Fig. 5, a comparison of the total e^+e^- mass spectrum calculated with the rates of SYZ and RUBW with the data is shown. Results for the SYZ rates with and without baryons are virtually indistinguishable from each other, despite the fact that significant enhancements were found below $M_{e^+e^-} < 400$ MeV. However, in this mass region, the Dalitz decay backgrounds, particularly those from $\eta \rightarrow \gamma e^+e^-$ and $\omega \rightarrow \pi^0 e^+e^-$, are an order of magnitude larger than the thermal yields and entirely mask the baryonic contributions. Thus, the differences in the total spectra are negligible for matter with and without baryons. The RUBW rates, being larger than those of SYZ in the region below the ρ -mass, lead to yields that are distinguishable from the case without baryons. It is clear from this comparison that accounting for the CERES data necessitates either substantial in-medium modifications, of magnitudes larger than so far considered, of the e^+e^- sources, or the presence of hitherto unidentified additional sources. The theoretical justification of such strong modifications or the existence of additional sources remains an open task.

We turn now to select comparisons with earlier works, in which the RUBW and SYZ rates have been used to confront the CERES data. Based on a schematic model for both the geometry and evolution of the fireball comprised of only hadrons from the beginning to the end of its evolution, it has been reported in Refs. [12,14] that the CERES data can be accounted for by using the rates reported there. Some relevant global features of these calculations are an initial temperature of 170 MeV, $T_f \cong 122$ MeV, and a lifetime of 15 fm/c [14]. In addition, a pion chemical potential was also employed at freeze-out to reproduce the observed total pion-to-baryon ratio. To make an appropriate comparison,

we performed a calculation using the EOS labeled EOS H, in which only hadronic degrees of freedom were admitted, with the initial conditions labeled IS 1 in Ref. [27]. To achieve good fits to hadronic data, an initial temperature of 270 MeV and a freeze-out temperature of 140 MeV were required. In this case, the lifetime of the center of the fireball was 12 fm/c (see the bottom panel of Fig. 2). The resulting e^+e^- spectra are virtually identical to those shown in Fig. 5 for the EOS with $T_c = 200$ MeV. For both EOSs with $T_c = 200$ and 165 MeV, the system evolves through the QGP, mixed, and pure hadron gas phases. For $T_c(T_f) = 200(140)$ MeV and 165(120) MeV, the total lifetimes of the center of the fireball are $\cong 11(14)$ fm/c, and the lifetimes in the pure hadron gas phase are $\cong 8(6.5)$ fm/c. In view of the inherent differences between hydrodynamic and schematic models, particularly those related with local versus global thermal equilibrium, chemical equilibration, and flow effects, a one-to-one comparison of these global quantities with those of the schematic model may be misleading. We wish to note, however, that in hydrodynamic calculations, the observed rapidity and transverse momentum spectra of the hadrons are also reproduced, in addition to the total pion-to-baryon ratio.

Our results are in qualitative agreement with those of SYZ, who also employed a schematic model for the expanding matter and concluded that the contributions from baryons cannot fully account for the reported excess in the data. This agreement, however, is mostly due to the magnitudes of the microscopic rates, which are considerably smaller than those of RUBW, particularly around $M_{e^+e^-} = 500$ MeV. The main conclusion that emerges from our calculations is that the e^+e^- spectra are relatively insensitive to the EOS for initial conditions that fit the observed hadronic spectra. In all cases considered here, the calculated results fall below the data around $M_{e^+e^-} = 500$ MeV by a factor of about 2-3.

To summarize, we have calculated e^+e^- emission in Pb+Au collisions at 158 AGeV/c using two different dielectron production rates within the framework of hydrodynamics. The rates calculated by SYZ include baryonic contributions arising from pion-nucleon interactions and those of RUBW account for additional in-medium modifications, which leads to a substantial broadening of the ρ -meson spectral function. We found that the additional con-

tributions due to baryons in the rates of SYZ give modest contributions, but mainly at low values of invariant mass where the spectrum is dominated by background decays. The final dielectron spectra with and without baryonic contributions are thus almost identical. On the other hand, the larger ρ -width in the rates of RUBW leads to comparatively larger yields in the 300–600 MeV mass region, but the enhancement still falls short of the enhancement observed in the data.

Several important theoretical issues remain to be resolved. The most prominent of these are: (1) The elementarity of a resonance when its in-medium width becomes substantially larger than its vacuum width, as found, for example, in the approach of RUBW. In many similar instances, multi-particle multi-hole excitations have been found necessary to account for the data. Closely connected with this is the extent to which collectivity, as implied in the resummations employed by RUBW, or as advocated in Ref. [26], is retained in high energy heavy-ion collisions in which the motion of all particles is highly randomized. (2) A comparison of our results with those of a transport approach to the space-time evolution of matter, in which equivalent, if not better, fits to the data have been reported, raises the issues of (i) whether a proper treatment of substantially broadened resonances in a transport description has been achieved, and (ii) whether the assumption of local chemical equilibrium in a hydrodynamic approach is adequate to treat the observables in high energy heavy-ion collisions.

Our calculations also highlight the need to pin down e^+e^- contributions from vector meson decays after freeze-out solely from experiments, independently of theory. Evidently, e^+e^- yields from the decay of the ω - and ϕ -mesons are sensitive to the freeze-out temperature in hydrodynamic calculations. In a sequential scattering approach, the ω and ϕ yields will depend upon the efficacy with which ωN and ϕN absorption processes deplete their primordial abundances [33]. Clearly, data with an improved mass resolution in the mass region of the ω - and ϕ -mesons, especially at different bombarding energies and for different projectile and target masses, are sorely needed to distinguish between competing theoretical scenarios. Since the mass shifts of these particles are expected to be small [34], accurate

data in this mass region will be of great advantage in calibrating the different models of space-time evolution. The establishment of such a standard candle will be particularly important in upcoming RHIC experiments, as it enables the disentanglement of hadronic versus sub-hadronic contributions to be placed on a firm footing.

We are particularly thankful to numerous intense discussions with G.E. Brown and other members and visitors of the Nuclear Theory Group at SUNY, Stony Brook. We gratefully acknowledge the help provided by R. Rapp, J. Steele, and I. Zahed concerning dilepton rates in the presence of baryons. Special thanks are due to P.V. Ruuskanen and J. Sollfrank for a careful reading of the paper, and to Axel Drees who provided us with the preliminary '96 CERES data and helped us to put the '95 CERES data in perspective. P.H.'s work is supported by the Academy of Finland grant 27574. The research of M.P. is supported by the grant DOE-FG02-88ER-40388.

REFERENCES

- [1] See e.g., Quark Matter'96, Nucl. Phys. **A610**, (1996).
- [2] G. Agakichiev et al., Phys. Rev. Lett. **75**, 1272 (1995); Nucl. Phys. **A610**, 317 (1996); Phys. Lett. **422B**, 405 (1998).
- [3] A. Drees Nucl. Phys. **A610**, 536 (1996); Nucl. Phys. **A630**, 449 (1998).
- [4] B. Lenkeit, INPC 98, Paris, Aug 24-28, 1998; see also B. Lenkeit, Doctoral Thesis, University of Heidelberg, 1998.
- [5] J. Cleymans, J. Fingberg, and K. Redlich, Phys. Rev. D **35**, 2153 (1987).
- [6] C. Gale and J.I. Kapusta, Nucl. Phys. **B357**, 65 (1991).
- [7] C. Gale and P. Lichard, Phys. Rev. D **44**, 2774 (1994); Phys. Rev. D **49**, 3338 (1994).
- [8] P. Lichard, Phys. Rev. D **49**, 5812 (1994); private communication.
- [9] C. Gale, in *Physics and Astrophysics of Quark-Gluon Plasma*, (Narosa Publishing House: New Delhi), 1998, eds. B.C. Sinha, D.K. Srivastava, and Y.P. Viyogi, p 360.
- [10] J.V. Steele, H. Yamagishi, and I. Zahed, Phys. Lett. **384B**, 255 (1997); Phys. Rev. D **56**, 5605 (1997); see also Z. Huang, Phys. Lett. **361B**, 131 (1995).
- [11] G. Chanfray, R. Rapp, and J. Wambach, Phys. Rev. Lett. **76**, 368 (1996).
- [12] R. Rapp, G. Chanfray, and J. Wambach, Nucl. Phys. **A617**, 472 (1997).
- [13] R. Rapp, M. Urban, M. Buballa, and J. Wambach, Phys. Lett. **417B**, 1 (1998).
- [14] R. Rapp, Proc. of 33rd Rencontres de Moriond on “QCD and High Energy Hadronic Interactions”, Les Arcs (France), March 21-28, 1998, nucl-th/9804065.
- [15] F. Klingl and W. Weise, Nucl. Phys. **A606**, 329 (1996); F. Klingl, N. Kaiser, and W. Weise, Nucl. Phys. **AA624**, 527 (1997).

- [16] C. Song, V. Koch, S.H. Lee, and C.M. Ko, *Phys. Lett.* **366B**, 379 (1996).
- [17] B. Friman and H.J. Pirner, *Nucl. Phys.* **A617**, 496 (1997).
- [18] W. Peters, M. Post, H. Lenske, S. Leupold, and U. Mosel, *Nucl. Phys.* **A632**, 1 (1998).
- [19] V.L. Eletsky and J.I. Kapusta, *nucl-th/9810052*.
- [20] G.Q. Li, C.M. Ko, and G.E. Brown, *Phys. Rev. Lett.* **75**, 4007 (1995); *Nucl. Phys.* **A606**, 568 (1996).
- [21] W. Cassing, W. Ehehalt, and C.M. Ko, *Phys. Lett.* **363B**, 35 (1995).
- [22] E.L. Bratkovskaya and W. Cassing, *Nucl. Phys.* **A619**, 413 (1997); W. Cassing, E.L. Bratkovskaya, R. Rapp, and J. Wambach, *Phys. Rev. C* **57**, 916 (1998).
- [23] J. Sollfrank, P. Huovinen, M. Kataja, P.V. Ruuskanen, M. Prakash, and R. Venugopalan, *Phys. Rev. C* **55**, 392 (1997).
- [24] C.M. Hung and E.V. Shuryak, *Phys. Rev. C* **56**, 453 (1997).
- [25] G.E. Brown and M. Rho, *Phys. Rev. Lett.* **66**, 2720 (1991).
- [26] G.E. Brown, G.Q. Li, R. Rapp, M. Rho, and J. Wambach, *Acta. Phys. Polonica*, **29**, 2309, (1998).
- [27] P. Huovinen, P.V. Ruuskanen, and J. Sollfrank, *nucl-th/9807076*.
- [28] J. Sollfrank, P. Huovinen, and P.V. Ruuskanen, *Heavy Ion Physics* **5**, 321 (1997).
- [29] J. Sollfrank, P. Huovinen, and P.V. Ruuskanen, *Euro. Phys. J. C*, in press, (nucl-th/9801023).
- [30] P.G. Jones et al. (NA49 collaboration), *Nucl. Phys.* **A610**, 188c (1996); P. Jacobs et al. (NA49 collaboration), in *Physics and Astrophysics of Quark-Gluon Plasma*, (Narosa Publishing House: New Delhi), 1998, eds. B.C. Sinha, D.K. Srivastava, and Y.P. Viyogi, p 248.

- [31] I. Ravinovich et al. (CERES Collaboration), Nucl. Phys. **A638**, 159c (1998)
- [32] V. Friese et al. (NA49 Collaboration) J. Phys. G **23**, 1837 (1997).
- [33] M. Berenguer, H. Sorge, and W. Greiner, Phys. Lett. **332B**, 15 (1994).
- [34] E.V. Shuryak and V. Thorsson, Nucl. Phys. **A536**, 732 (1992).

FIGURES

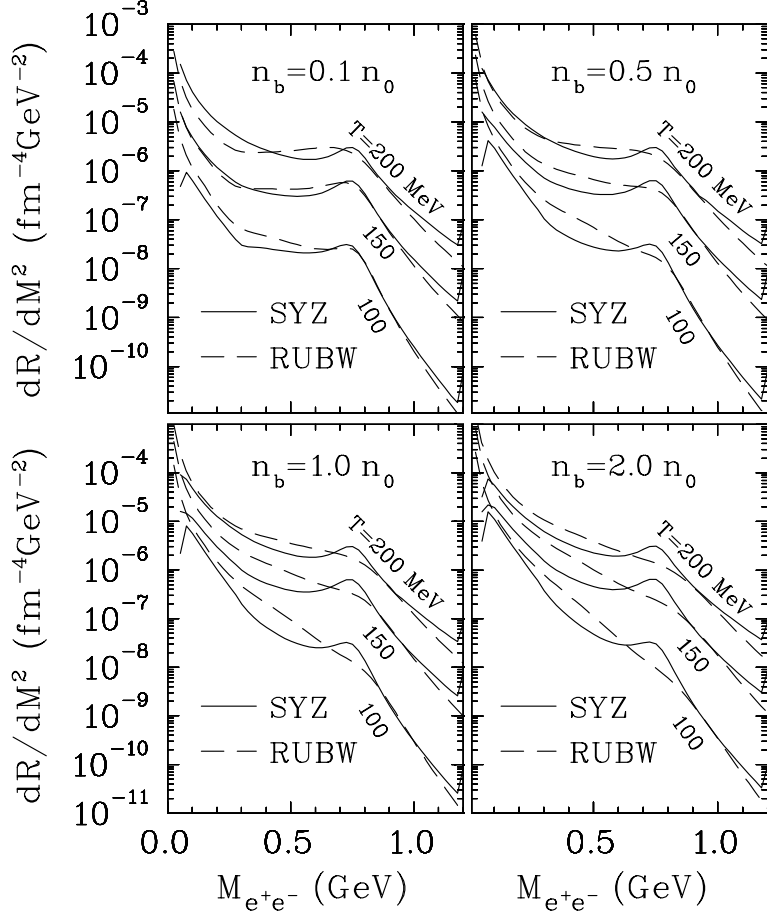


FIG. 1. The e^+e^- production rates at different temperatures and baryon densities versus pair invariant mass. The solid lines are results of Steele, Yamagishi, and Zahed (SYZ) and the dashed lines are those of Rapp, Urban, Buballa, and Wambach (RUBW).

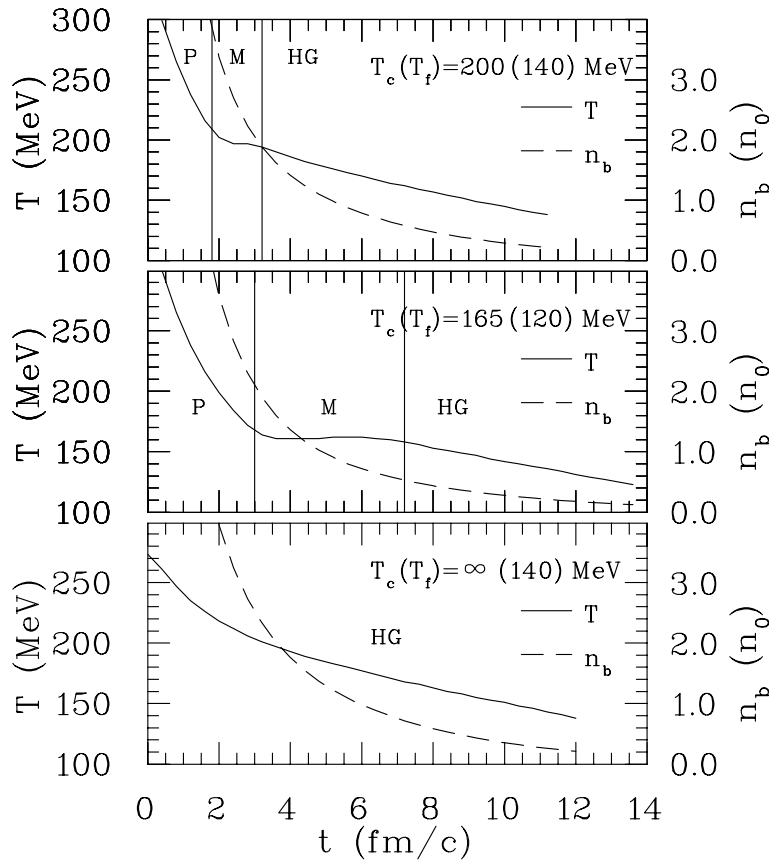


FIG. 2. Temperature (left scale) and baryon density in units of the nuclear equilibrium density (right scale) in the center of the fireball as a function of time. The symbols P, M, and HG denote the plasma, the mixed, and hadron gas phases, respectively. The top (middle) panel shows results for an EOS with $T_c = 200(165)$ MeV and the bottom panel for a hadronic EOS without a phase transition. Equivalent fits to the hadronic spectra are obtained at the indicated freeze-out temperatures of $T_f = 120$ and 140 MeV.

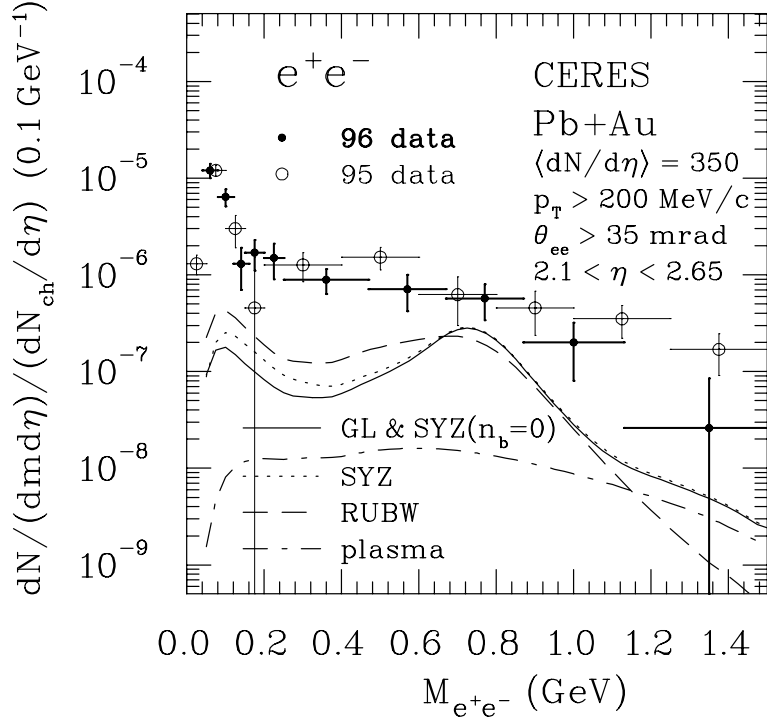


FIG. 3. Dielectron yields from the hadronic part and plasma part of the fireball for $T_c(T_f) = 200(140)$ MeV. Solid lines are results for matter without baryons and are obtained by using the rates of SYZ which agree with those of Gale and Lichard (GL). Results in matter with baryons (short-dashed lines from the SYZ rates and long-dashed lines from the rates of RUBW) are also shown. Kinematic cuts and detector resolution are incorporated.

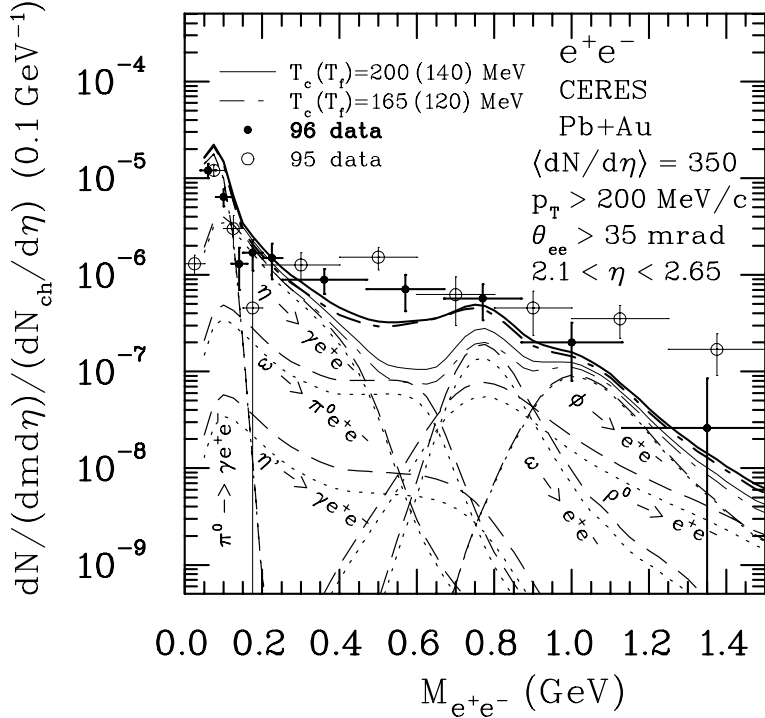


FIG. 4. Background contributions from meson decays after freeze-out of the hydrodynamical evolution for $T_c(T_f) = 200(140)$ MeV and $165(120)$ MeV, respectively, which give equivalent fits to the hadronic spectra. In all cases, the higher yields refer to $T_c(T_f) = 200(140)$ MeV. The thin solid (dashed) line shows the total background. The thick solid (dashed) line shows the sum of background and fireball contributions calculated using the RUBW rates. Kinematic cuts and detector resolution are incorporated.

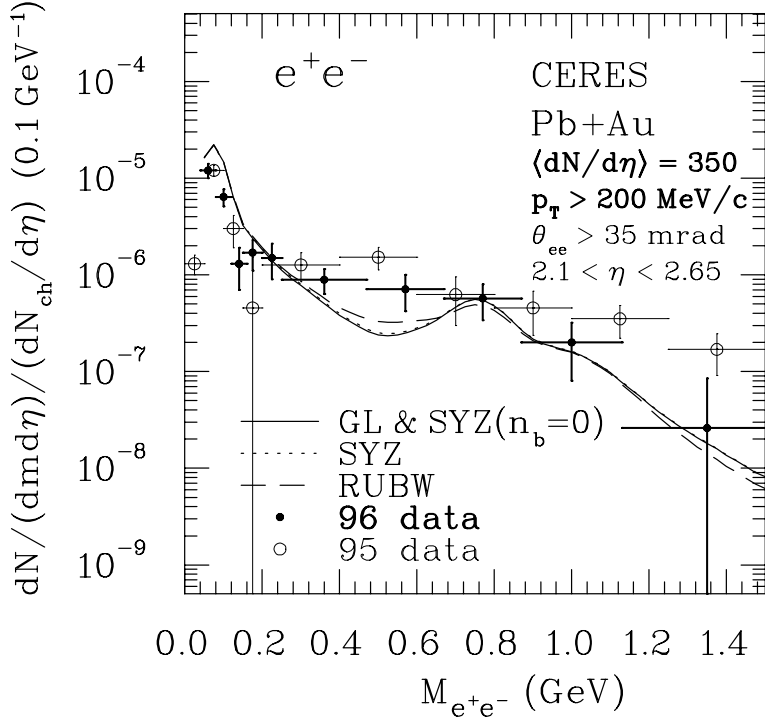


FIG. 5. Calculated total dielectron mass spectra for $T_c(T_f) = 200(140)$ MeV compared with the CERES data. Solid lines are results for matter without baryons and are obtained by using the rates of SYZ which agree with those of GL. Results in matter with baryons (short-dashed lines from the SYZ rates and long-dashed lines from the rates of RUBW) are also shown. Kinematic cuts and detector resolution are incorporated.